

# Study and Control of Phase Morphology in Liquid Crystal Polyester–Poly(alkylene Terephthalate) Blends

J. -F. CROTEAU and G. V. LAIVINS,\* *Centre de Recherche en Sciences et Ingénierie des Macromolécules, Département de Chimie, Université Laval, Sainte-Foy, Québec, Canada G1K 7P4*

## Synopsis

Scanning electron microscopy (SEM) reveals that the morphologies of poly(hexamethylene terephthalate) (PHMT) and poly (*p*-oxybenzoate co-ethylene terephthalate) (LCP6/4) blends are biphasic. When LCP6/4 is the minor component, liquid crystalline domains are embedded in the matrix. The reaction in the melt between the polymers apparently increases the adhesion of the matrix to the embedded domains. As the reaction proceeds, the chemical composition of the matrix progressively becomes modified. High reaction temperatures, small particle size, mixing coupled with particle dispersion and high LCP6/4 content in the mixture promote the melt reaction and decrease the PHMT content in the polymer formed. At 260°C, the coaddition of di-*n*-octadecyl phosphite (DNOP) at a 2% weight fraction with PHMT and LCP6/4 inhibits the reaction between the polymers for 2 h.

## INTRODUCTION

The demands that materials attain some critical balance between properties which may be inherently contradictory has focused attention on polymeric blends and processing technology. Blends of liquid crystalline polymers (LCP) (high tensile strength but buckle under compression) with conventional thermoplastic resins can have high tensile and compressive strengths.<sup>1</sup> Although the individual component polymers are chosen so that they collectively fulfill the requirements; when blended, the properties of the component polymers are not always additive. Factors as the interactions between the polymer–polymer segments, the phase morphology (size, shape, and dispersion of the phases) the nature and degree of adhesion at the interface of the phases intervene and effect the property relationships in polyblends.

Blends where thermoplastic resins are reinforced by thermotropic liquid crystalline polymers mixed in the melt, upon cooling spontaneously form *in situ* composites.<sup>2–4</sup> Liquid crystalline polymers form ordered fluids with few entanglements and thus facilitate the processing of the resin by lowering the melt viscosity. Upon cooling, the liquid crystalline polymer solidifies forming fibrillar structures which reinforce the thermoplastic resin. Thus blends of liquid crystalline polymers and thermoplastics form light weight, high strength materials. At present, only a few systems have been studied.<sup>3–20</sup>

\*Present address: Pulp and Paper Research Institute of Canada, 570 John's Boulevard, Pointe Claire, PQ, Canada H9R 3J9.

Preliminary investigations have indicated that the blend of a resin and liquid crystalline polymer is a multiphased material with a complex morphology. When the LCP is the minor phase elongated liquid crystalline domains or fibrils with diameter of 1–10  $\mu\text{m}$  are embedded in the resin. A network structure forms at higher LCP contents.<sup>3–10</sup> Studies examining blends of LCP and coiled polymers for evidence of segmental miscibility in the amorphous phase<sup>4,7–15</sup> and crystalline phases<sup>8,13,14,16–18</sup> have been initiated.

In a complementary investigation the apparent miscibility between poly(hexamethylene terephthalate) (PHMT) and a copolyester of acetoxybenzoic acid (p-OB) and poly(ethylene terephthalate) (PET) was attributed to a reaction which occurred in the melt.<sup>21</sup> This reaction between PHMT and the copolyester may provide a mechanism to create chemical interactions at the interface of the liquid crystalline domains and the surrounding matrix. Blends of PHMT and the copolyester could be pushed to the "edge of miscibility" via the melt reaction. Blends on the borderline of compatibility should have finely dispersed phases, low melt interfacial tension, and high interfacial adhesion; all of which may impart advantageous properties.<sup>22–24</sup>

The research objectives of this investigation are to study the relationships between the processing and morphology of a blend of PHMT and the p-OB/PET copolyester. A rich variety of morphological features which are sensitive to the processing conditions should be exhibited by PHMT-p-OB/PET copolyester blends. The morphology of blends of PHMT with the p-OB/PET copolyester are investigated using differential scanning calorimetry (DSC), wide angle X-ray scattering (WAXS), and scanning electron microscopy (SEM). The morphology of PHMT-copolyester extrudates in relation to blend composition, mixing rate, and temperature are examined with SEM. The effect of the blend preparation technique (dissolution/coprecipitation or injection moulding) on the reaction is analyzed. The processing conditions required to limit and control the reaction are shown. The influence of the reaction on the adhesion between the matrix and the embedded liquid crystalline domain is qualitatively described from SEM micrographs.

## EXPERIMENTAL

### Blend Preparation

PHMT (Eastman Chemicals) and a p-OB/PET copolyester (Tennessee Eastman Kodak) with trade name X7G and intrinsic viscosity of 0.95 in 60:40 (by volume) phenol-tetrachloroethane at 25°C were used without further purification. The copolyester with a ratio of p-OB to PET units of 6 to 4 is referred to as LCP6/4 in this paper. (It forms a liquid crystalline phase when heated above 250°C.) Publications detailing the synthesis and characterization of LCP6/4 are numerous.<sup>25–33</sup> The characterization of PHMT can also be found in the literature.<sup>34</sup>

A mixture of 0.35 g PHMT and 0.15 g LCP6/4 powders was dissolved in 50 mL of 2-chlorophenol (Aldrich) at 60°C. The polymers were coprecipitated into 500 mL of methanol, filtered, and washed with boiling methanol. The

TABLE I  
 PHMT Weight Fraction in Binary PHMT-LCP6/4 Mixtures Introduced into the Extruder  
 at 260°C, Mixing Time, Percentage of the Extracted Extrudate  
 Recovered in the Chloroform Extract

PHMT-LCP6/4 extrudate	Mixing time (min)	% of extrudate recovered as extract
67-33	180	88
50-50	150	68
33-67	160	48
20-80	160	40
50-50 <sup>a</sup>	30	53
50-50 <sup>a</sup>	120	53
50-50 <sup>a</sup>	300	63

<sup>a</sup>Extrudates doped with 2% of DNOP.

coprecipitated mixture was dried at 80°C with dynamic evacuation for 3 weeks.

Samples of 67-33 and 50-50 (PHMT-LCP6/4) powders and 67PHMT-33LCP6/4 mixtures doped with 0.6% (by weight) di-*n*-octadecyl phosphite (DNOP) (Aldrich) were simultaneously introduced in a single screw Mini-Max CS-183 Moulder (Custom Scientific Instruments). The preheated cavity was the vessel for the reaction which occurred in the melt during mixing at 100 rpm. The reaction was stopped abruptly when the mixture was injected into a cold mould.

The extruded blends from the molder were extracted with chloroform for 24 h in a Soxhlet apparatus. The insoluble residue remaining in the thimble was a white fibrous material. The extract which contained the chloroform soluble material was rotary evaporated to dryness leaving a slightly discolored opaque film. The PHMT weight fraction in the PHMT-LCP6/4 mixture introduced into the moulder, mixing time and percentage of the extrudates recovered in the chloroform extract are given in Table I.

## Measurements

### *Differential Scanning Calorimetry (DSC)*

A Perkin-Elmer DSC 4 apparatus was used to measure the thermal transitions in coprecipitated PHMT-LCP6/4 mixtures, PHMT-LCP6/4 extrudates, and extracted fractions. Prior to registering a thermogram, samples were encapsulated in aluminium pans, equilibrated for 5 min at 200°C, and then crystallized for 15 min at 115°C. All samples were heated from -20 to 200°C at a rate of 20°C/min under a nitrogen atmosphere. A registered scan of the baseline was subtracted from the measured thermogram to minimize artifacts due to variations in the baseline, and every scan was repeated at least once more to verify the reproducibility of the measurement. The  $T_g$  is taken at half height in the change in energy absorbed during the transition. The temperature which corresponds to the high temperature end of the melting endotherm is the reported  $T_m$ .

*X-Ray Data*

A PHMT sample and 67PHMT-33LCP6/4 extrudates doped with 0.6% DNOP were exposed to Ni-filtered,  $\text{CuK}\alpha$  radiation with intensity of 8.0 kW emitted from the rotating anode source of a Rigaku Rotaflex RU 200 diffractometer. The intensity of the scattered radiation over the Bragg angles of 3-53° during a single sweep was measured with a scintillation counter. The equatorial axis was scanned at a rate of 5°C/min in steps of 0.1°C. Measurements were in the symmetric transmission geometry with 2 mm diameter collimation of the point focus source. The sample to receiving slit distance was 170 mm.

*Nuclear Magnetic Resonance Spectroscopy (NMR)*

The proton NMR spectra of the copolymers extracted from the extrudates dissolved in deuterated chloroform were measured with a Fourier transform Varian XL 200 NMR spectrophotometer operating at 200 MHz.

*Scanning Electron Microscopy (SEM)*

PHMT-LCP6/4 extrudates (cross-sectional area of  $5 \times 1$  mm) and the insoluble residue of chloroform extracted extrudates were immersed in liquid nitrogen and fractured across the flow direction in flexure. A 50  $\mu\text{m}$  thick gold palladium amalgam coating was sputtered onto the fracture surfaces to render them conductive. Micrographs depicting the morphological features of the extrudates were taken with a JEOL JSM-T220 scanning electron microscope operating at an accelerating voltage of 15 kV with a Polaroid camera attachment.

**RESULTS AND DISCUSSION****Coprecipitated Mixtures**

Coprecipitated mixtures of PHMT and LCP6/4 from 2-chlorophenol solution into methanol form mechanical mixtures without interactions between the polymers. As a consequence of a reaction that occurs in the melt during a thermal pretreatment, interactions develop between the components.<sup>21</sup> The DSC thermograms indicate two  $T_g$ 's: one which corresponds to that of LCP6/4 and the second which occurs in a temperature range above that of bulk PHMT. The chemical composition of the matrix polymer may be controlled by the reaction parameters (e.g., duration and temperature).

DSC thermograms of coprecipitated mixtures of 70PHMT-30LCP6/4 reacted at 226, 260, and 300°C were measured. The variation in the glass transition temperature of the matrix phase with the reaction time are given in Figure 1. The data at temperatures of 226, 260, and 300°C are represented by triangles, circles, and squares, respectively. The  $T_g$  of the matrix polymer of a 70PHMT-30LCP6/4 mixture following 2 h at 226°C (not shown) is  $17.6 \pm 1^\circ\text{C}$ . The melt reaction initially progresses very rapidly at all three temperatures. At 300°C, the polymer with an equilibrium composition forms in about 2 min but requires 10 min at 226°C. (It is supposed that the  $T_g$  increases as the composition of the polymer becomes poorer in PHMT; the variation in the  $T_g$

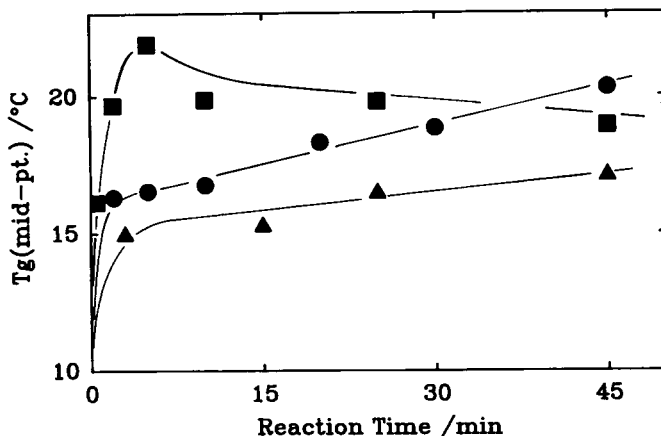


Fig. 1. The variation of the glass transition temperature with reaction time for 70PHMT-30LCP6/4 coprecipitated mixtures. The data are represented by triangles at 226°C, circles at 260°C, and squares at 300°C. The samples were recrystallized at 115°C for 15 min following the reaction.

is a rough measure of the progression of the reaction.) At 260°C (following 5 min when a jump in the  $T_g$  occurs) the  $T_g$  increases regularly with reaction time. Once the groups in close proximity have reacted, the reaction is diffusion controlled and slows down. At 226°C, following the initial reaction, the viscosity of the mixture hinders the diffusion and essentially limits the reaction. The slight decrease in the  $T_g$  with reaction time at 300°C is attributed to polymer degradation. The equilibrium composition of the polymer is temperature-dependent when diffusion effects are neglected. For the given PHMT-LCP6/4 mixture, the equilibrium composition is poorer in PHMT at elevated temperatures.

The melting temperature  $T_m$  and the change in enthalpy,  $\Delta H_m$ , per gram of the blend associated with the melting behavior measured by scanning calorimetry of the 70PHMT-30LCP6/4 coprecipitated mixtures at reaction temperatures of 226, 260, and 300°C are compiled in Table II. The  $T_m$  of each matrix phase is slightly lower than that of bulk PHMT;  $T_m$  of  $155 \pm 2^\circ\text{C}$ . The  $T_m$  values vary between 149 and 154°C and are insensitive to the reaction

TABLE II  
Melting Temperature and Change in Enthalpy Associated with the Melting of the Crystalline Matrix Phase of 70PHMT-30LCP6/4 Coprecipitated Mixtures Reacted at 226, 260, and 300°C

Time (min) 226°C	$T_m$ (°C)	$\Delta H^a$ (cal g <sup>-1</sup> )	Time (min) 260°C	$T_m$ (°C)	$\Delta H^a$ (cal g <sup>-1</sup> )	Time (min) 300°C	$T_m$ (°C)	$\Delta H^a$ (cal g <sup>-1</sup> )
4	154.0	7.1	2	152	6.9	0.5	153	7.7
15	152.0	6.8	5	150	7.5	2.0	152	7.9
25	151.0	6.9	10	149	7.05	5.0	153	7.8
45	149.0	7.8	20	149	6.9	10.0	149	7.7
120	151.5	6.65	30	149	7.1	25.0	147	7.9
			45	152	7.3	45.0	142	7.5

<sup>a</sup> Per gram of mixture.

time. No significant variation in the  $T_m$  nor in the  $\Delta H_m$  values occurs for the coprecipitated mixtures at 226 or 260°C. (However, a mixture reacted at 300°C for 45 min melts at 142°C.) Progression of the reaction with the formation of phases poorer in PHMT would lower the  $T_m$  and decrease the  $\Delta H_m$  value while the  $T_g$  should exhibit the reverse trend. A trend in the  $\Delta H_m$  values with reaction time is not observed while the  $T_g$  decreases slightly. However, the trends at 300°C; the large observed lowering of the  $T_m$  coupled with a  $T_g$  decrease are consistent with the hypothesis of polymer degradation for long reaction times at elevated temperatures.

The  $\Delta H_m$  values apparently are independent of the reaction time at each temperature; however, the average  $\Delta H_m$  value increases from 6.9 through 7.1 to 7.8 cal/mixture when the reaction temperature is increased from 226–260° to 300°C. From the values it is tempting to suggest that the cohesive lattice energies of the polymers formed at 300°C ( $\Delta H_m$  of 7.8) are greater than those formed at 226°C ( $\Delta H_m$  of 6.9). However, the  $\Delta H_m$  values are per gram of mixture not of matrix polymer. At low reaction temperatures the reaction yield is low. As a consequence of the lower reaction yields at 226°C, the total change in enthalpy due to the melting of crystals is smaller than at 300°C. The  $\Delta H_m$  values should be normalized to the number of lattice cells in the crystalline phase which melt, not the quantity of mixture nor bulk PHMT.

Normally the inclusion of a second crystallizable sequence into a semicrystalline polymer disrupts the unit cell and lowers the cohesive lattice energy. Consequently, the copolymers formed have lower  $T_m$  and lower  $\Delta H_m$  values than the initial homopolymer.<sup>35</sup>

### Extrudates

The variation of the  $T_g$  of the matrix phase of binary PHMT-LCP6/4 extrudates with mixing time in a preheated chamber is shown in Figure 2. The data for 67PHMT-33LCP6/4 extrudates mixed at 226 and 260°C are given by

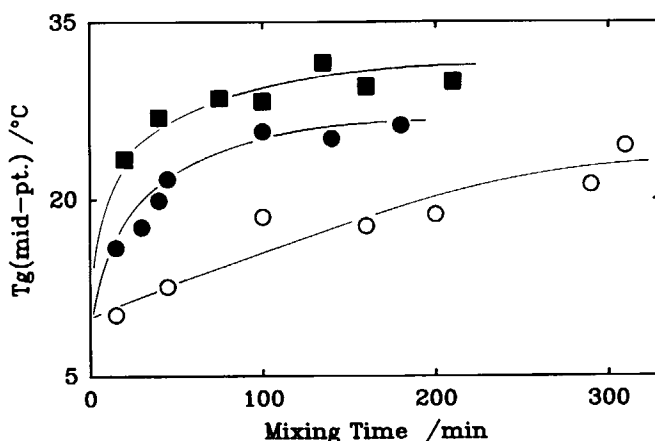


Fig. 2. The variation of the  $T_g$  of the matrix of binary PHMT-LCP6/4 extrudates with mixing time. The data for 67PHMT-33LCP6/4 extrudates mixed at 226°C are given by open circles and by filled circles for those mixed at 260°C, and by filled squares for 50-50 extrudates mixed at 260°C.

TABLE III  
Melting Temperature and Change in Enthalpy of the Melting of the Crystalline Matrix  
Phase of Binary PHMT-LCP6/4 Extrudates Mixed at 226 and 260°C

67PHMT-33LCP6/4 (226°C)			67PHMT-33LCP6/4 (260°C)			50PHMT-50LCP6/4 (260°C)		
Time (min)	$T_m$ (°C)	$\Delta H^a$ (cal g <sup>-1</sup> )	Time (min)	$T_m$ (°C)	$\Delta H^a$ (cal g <sup>-1</sup> )	Time (min)	$T_m$ (°C)	$\Delta H^a$ (cal g <sup>-1</sup> )
15	153.0	5.3	15	152.0	8.4	20	151	5.6
45	152.0	6.0	30	153.0	6.9	40	152	5.2
100	151.0	7.6	40	152.0	7.4	75	145	5.6
160	150.5	7.5	45	153.0	7.8	100	146	5.6
200	150.0	7.4	100	154.5	8.6	135	145	5.6
290	148.5	7.6	140	150.0	8.1	160	144	5.8
310	147.0	6.85	180	148.0	7.65	210	142	5.2
480	148.0	7.5						

<sup>a</sup> Per gram of extrudate.

the open and filled circles, respectively. The filled squares represent the data for 50PHMT-50LCP6/4 extrudates mixed at 260°C. At 260°C the reaction initially proceeds rapidly and attains an equilibrium state within 90 min. The reaction at 226°C progresses at a slower rate and the steady state requires at least 6 h. The  $T_g$  of the 67PHMT-33LCP6/4 extrudate mixed for 8 h at 226°C (not shown) is  $23 \pm 1^\circ\text{C}$ . The reaction rate does not change significantly with composition of the initial mixture. At 260°C, the reactions in the 67PHMT-33LCP6/4 and the 50-50 mixtures attain an equilibrium state in similar times (the  $T_g$  of the matrix polymers are constant). The equilibrium composition varies with the composition of the initial mixture. The polymer formed from the the 50PHMT-50LCP6/4 reaction mixture has a higher  $T_g$  ( $\approx 31^\circ\text{C}$ ) and thus is poorer in PHMT than the equilibrium polymer formed in the 67PHMT-33LCP6/4 mixture whose  $T_g$  is  $26^\circ\text{C}$ . The variation of the  $T_g$  with reaction time in the 67PHMT-33LCP6/4 extrudates at 226 and 260°C do not establish a clear dependence of the equilibrium polymer content on the mixing temperature. Although the  $T_g$  of the matrix of the extrudates mixed at 226°C approaches a constant value, it nevertheless gradually increases for prolonged reaction times, and may eventually attain the same  $T_g$  as in the equilibrium extrudate at 260°C.

The melting point and change in the enthalpy associated with the melting behavior per gram of blend of the crystalline phase for binary PHMT-LCP6/4 extrudates mixed at 226 and 260°C are compiled in Table III. The melting endotherm of the crystalline phase of binary PHMT-LCP6/4 extrudates mixed at 226 or 260°C resembles that observed for the coprecipitated mixtures at these temperatures. In each of the mixtures a regular decrease in the  $T_m$  occurs with mixing time which becomes fairly pronounced for the 50PHMT-50LCP6/4 extrudates. Apparently the melt reaction progresses to a further degree in the 50-50 mixtures. The lattice structure is destabilized and thus the  $T_m$  decreases. Consequently, a substantial  $T_m$  lowering occurs with the 50PHMT-50LCP6/4 extrudates. The change in enthalpy of melting values when normalized to gram of polymer formed are expected to decrease

TABLE IV  
 PHMT Weight Fraction in Binary PHMT-LCP6/4 Mixtures Introduced into the Extruder at 260°C, Mixing Time, PHMT Content of the Extracted Polymer,  $T_g$ ,  $T_m$ , and Change in Enthalpy of Matrix Phase

PHMT-LCP6/4 extrudate	Mixing time (min)	PHMT content of extracted polymer	$T_g$ (°C)	$T_m$ (°C)	$\Delta H^a$ (cal g <sup>-1</sup> )
67-33	180	87	22	146	8.1
50-50	150	70	27	144	8.6
33-67	160	68	33	142	7.45
20-80	160	58	30	138	4.9

<sup>a</sup> Per gram of extracted material.

with mixing time. However, the lower cohesive lattice energy of the deformed unit cells is offset by an increasing reaction yield and a constant  $\Delta H_m$  value when normalized to the gram of blend (Table III) with mixing time is observed.

### Chloroform Soluble Extracts

The NMR spectrum of the extracted fraction shows that the matrix phase following the reaction has both hexamethylene and ethylene terephthalate sequences. With the hypothesis of a transfer of PET from LCP6/4, the PHMT content in the extracted polymers was calculated from the ratio of the integration curves corresponding to the absorption by the appropriate protons.<sup>21</sup> The weight fraction of PHMT in binary PHMT-LCP6/4 mixtures introduced into the molder at 260°C, mixing time, PHMT weight fraction in the extracted polymer, transition temperatures, and heat absorbed for the matrix phase transitions are compiled in Table IV. The equilibrium polymers contain less PHMT when the mixture introduced was rich in LCP6/4. The percentage of available PET transferred from LCP6/4 is lower for mixtures rich in this component. Some PET in LCP6/4 remains. This indicates that the reaction does not proceed until completion but attains an equilibrium state.

Although the  $T_g$  of the matrix phase appears to be relatively insensitive to changes in the PHMT content, the molar mass of the extracted polymers was not measured. It is probable that, as the reaction progresses, there is a concomitant decrease in the molar mass of the product polymers. (Generally the  $T_g$  of a polymer has a direct dependence on the molar mass. The variation of the  $T_g$  on the molar mass becomes pronounced in the low molar mass range.)<sup>36</sup> The glass transition of the extracted polymers occurs over a reduced temperature interval when compared with the temperature span for the glass transition in the equilibrium extrudate from which it was extracted. Additionally the  $T_g$  of the extracted polymer is slightly lower than that of the matrix of the extrudate. A slight expansion of the span for the glass transition and shift to higher temperatures upon blending with a second polymer is suggestive of limited mixing.

The  $T_m$  of the extracted polymers decreases regularly with LCP6/4 content in the mixture. Extracted polymers have  $T_m$  of 146°C and a PHMT content of



87% while those which contain 58% PHMT melt at 138°C. The  $T_m$  of the extracted polymer is close to the  $T_m$  of the crystalline phase of the PHMT-LCP6/4 extrudate from which it was extracted. The change in enthalpy upon melting decreases regularly with LCP6/4 content in the mixture. The reaction between PHMT and LCP6/4 gives semicrystalline polymers, and the ratio of gram of polymer formed to gram of PHMT originally introduced increases with LCP6/4 content. When normalized for the PHMT content, the  $\Delta H_m$  per gram of PHMT is fairly independent of the PHMT content in the extracted polymers because the normalization to gram of PHMT systematically introduces a larger error.

### Effect of Blending Technique on Reaction

The choice of blending technique (dissolution/coprecipitation or melting/injection molding) affects the reaction significantly. When dissolved, the polymers in solution are randomly distributed. Coprecipitation gives fine particles of the two polymers dispersed throughout the mixture. When heated, due to the close proximity of the reagents, an immediate and rapid reaction occurs in coprecipitated mixtures. It is virtually impossible to injection mold the coprecipitated mixtures without substantial reaction having occurred. However, the lack of further mixing limits the reaction. Thus the equilibrium composition is temperature-dependent. Conversely the reaction in the extruder is hindered by the slow mixing of the molten polymers; however, a greater control of the reaction is gained. The continuous mixing enables the reaction to progress and attain the equilibrium condition which does not occur when coprecipitated mixtures are heated. The composition of the polymers formed will be time-dependent but temperature-independent.

### PHMT-LCP6 / 4 Extrudates Doped with Di-*n*-Octadecyl Phosphite

In blends of poly(butylene terephthalate) (PBT) or PET and polycarbonate (PC), where transesterification reactions occur at elevated temperatures, the presence of residual concentrations of titanium derivatives in commercial terephthalate polymers catalyzes the exchange reaction.<sup>37-40</sup> (Titanium derivatives are catalysts in the polymerization of terephthalates.) Initially block copolymers are formed; however, for prolonged reactions redistribution occurs and the composition of the copolymers becomes statistical.<sup>24</sup> Thus either block or statistical copolymers can be formed by simply reacting two polyesters in an extruder and controlling the exchange reaction. Control of the exchange reaction could be gained by addition of an agent which complexes with the titanium derivatives. Addition of the complexing agent together with the polymers at the start of the processing would permit the preparation of nonreactive blends which could be injection-molded. Alternatively, the complexing agent could be added to the blend after the exchange reaction has progressed. The exchange reaction would stop in midcourse upon addition of the complexing agent. Vanadium or phosphorous compounds can prevent the randomization of block copolyesters.<sup>41,42</sup> At 260°C, the addition of 0.5% (weight fraction) of di-*n*-octadecyl phosphite (DNOP) or triphenyl phosphite to a PBT-PC blend inhibits the onset of the transesterification reaction for

more than 2 h.<sup>24,43</sup> The postulated mechanism is the formation of an octahedral titanium complex with the organic ligands of the phosphite derivatives.<sup>24</sup>

To investigate the influence of DNOP on the progress of the reaction in the PHMT-LCP6/4 melt at 260°C, mixtures of the components in a 1 : 1 weight ratio with 0.02 DNOP (weight fraction) were blended for 30, 120, and 300 min. The extrudates were extracted and the proton NMR spectrum of the soluble fraction was measured.

The weight fraction of the extrudates recovered as solubles was 0.53 for mixing times of 30 and 120 min and increased to 0.63 when mixed for 300 min. (The total PHMT and DNOP weight fraction originally in the mixtures was 0.52.) Naturally, the portion of the extrudate recovered as insolubles decreased during the reaction interval. The PHMT content in the soluble fraction was calculated from the NMR spectrum.<sup>21</sup> The soluble fraction of extrudates mixed for 30 and 120 min contains more than 93% PHMT. However, the reaction becomes significant in the extrudate mixed for 300 min and the PHMT content decreases to 77%. (Assuming complete transfer of PET to the soluble fraction, the PET content from 50PHMT-50LCP6/4 extrudates cannot exceed 29%.) The PHMT content of the chloroform soluble extract from an extrudate of a 50PHMT-50LCP6/4 mixture blended at 260°C without DNOP for only 30 min is 75%. Thus at 260°C the addition of 2% DNOP inhibits the reaction in the PHMT-LCP6/4 melt for a minimum of 2 h.

The variation of the  $T_g$  of the matrix phase of 67PHMT-33LCP6/4 extrudates doped with 0.6% DNOP with mixing time at 260°C is shown in Figure 3. As indicated by the gradual increase of the  $T_g$  with mixing time, the reaction progresses slowly. The reaction attains an equilibrium state after 10 h, at which time the composition of the extracted polymer is 73% PHMT. At 260°C the reaction in the absence of DNOP attains an equilibrium state after 90 min in 67PHMT-33LCP6/4 mixtures.

The melting temperatures and the change in enthalpy of the crystalline phase in the 67PHMT-33LCP6/4 extrudates doped with DNOP and mixed at

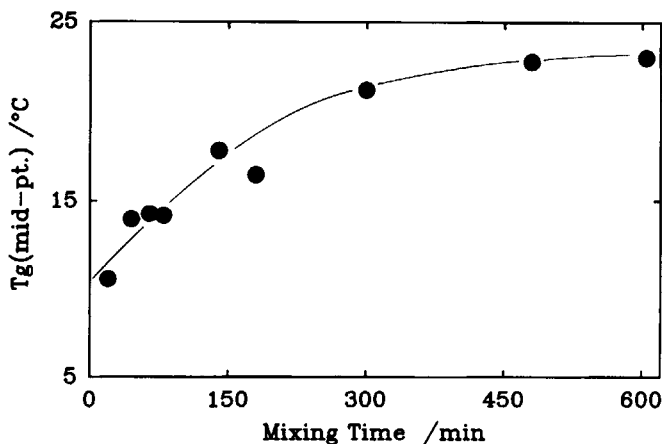


Fig. 3. The variation of the  $T_g$  of the matrix of 67PHMT-33LCP6/4 extrudates doped with 0.6% DNOP blended at 260°C with mixing time.

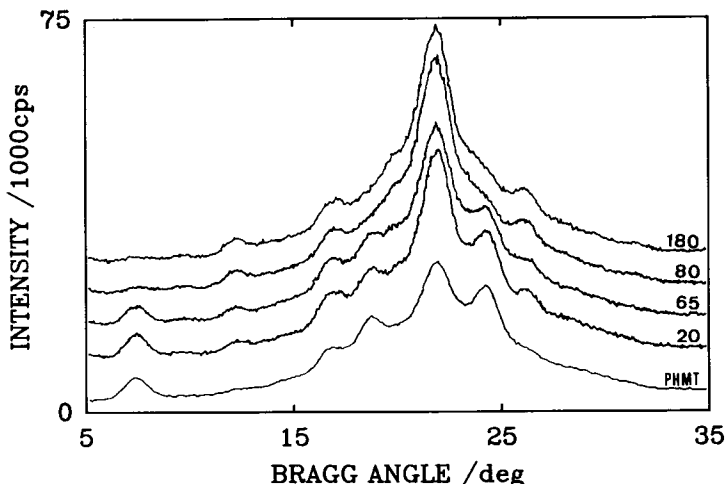


Fig. 4. The WAXS spectra of the non-LCP6/4 components in 67PHMT-33LCP6/4 extrudates doped with 0.6% DNOP mixed at 260°C and of bulk PHMT. The scattering due to LCP6/4 has been subtracted from each measured spectrum. The blending time for each mixture is indicated above the curve.

260°C for less than 300 min remain at their maximum values. However, when mixed for longer times (480 and 600 min), the  $T_m$  and  $\Delta H_m$  values begin to decrease. At 260°C, only after prolonged mixing does the reaction between PHMT and LCP6/4 significantly affect the crystalline phase in the extrudates doped with 0.6% DNOP.

The wide angle X-ray scattering pattern between the Bragg angles of 5° and 35° of PHMT and of 67PHMT-33LCP6/4 extrudates doped with 0.6% DNOP mixed at 260°C for 20, 65, 80, and 180 min are shown in Figure 4. The scattering due to the LCP6/4 component has been subtracted from the measured patterns for all the extrudates. The scattering pattern of the extrudates mixed for 20 and 65 min resemble that of bulk PHMT, indicating that the crystalline phase in the extrudates adopts the lattice structure of PHMT. (The presence of DNOP in the extrudates apparently does not distort the lattice structure.) Modifications of the lattice structure become evident in the extrudate mixed for 80 min; the peaks centered at Bragg angles of 7.3, 18.6, and 24.0° are no longer present, while peaks centered at Bragg angles of 12.2 and 26.2° appear and intensify. These latter peaks are not found in the pattern of unoriented bulk PHMT (lower curve). The WAXS patterns of 67PHMT-33LCP6/4 extrudates without DNOP blended at 260°C for 15 min exhibit similar crystal structure modifications.<sup>21</sup> As the crystal lattice is not deformed for the extrudates mixed for less than 80 min, the addition of 0.6% DNOP clearly inhibits the reaction.

### Extrudate Morphology

The fracture cross section (normal to the melt flow direction) of PHMT-LCP6/4 minitensile bar extrudates were examined using SEM. The complex flow fields in the polymeric mixtures as molten material is forced through a narrow orifice into a cold mold induces the development of a

skin-core morphology. The liquid crystalline domains in the skin region (near to the surface) have a more elongated shape and form sheetlike structures. As the skin layer is a minor fraction of the entire fracture cross section and is not representative of the bulk material, the micrographs selected for this paper depict the morphology in the "core" region.

The SEM micrographs of the fracture cross section of 67PHMT-33LCP6/4 extrudates mixed at 225 and 260°C which illustrate the temperature sensitivity of the extrudate morphology are shown in Figure 5. The micrographs of both extrudates depict a two-phase morphology with the minor component embedded in a matrix of the majority component. At 260°C, the shape of the embedded domains is needlelike whereas at 225°C the liquid crystal (LC) domains are spherically shaped. The presence of holes in the matrix (evidently left by pulled out LC domains) coupled with observation that many of the LC domains have tapered tips implies that the adhesion of embedded LC domains to majority phase at 260°C is only fair. (An absence of holes, evidence of pulled out LC domains, indicates excellent adhesion while pulled out rods with a flat cross section implies poor adhesion.) At 225°C, the domains are pulled out cleanly and leave holes in the matrix.

The series of micrographs shown in Figure 6 of the fracture cross section of PHMT-LCP6/4 extrudates mixed at 260°C illustrates the variation of the morphology with composition. When the LCP6/4 was the minor component in the mixture, the morphology of the extrudate has holes from the pulled out LC domains and needlelike LC domains projecting from the matrix. Additionally the LC domain size is independent of the LCP6/4 content in the mixture. The greater content of LCP6/4 in the mixture is reflected in the extrudates by an increased density of holes in the matrix and by an increased density of LC domains. Thus as the PHMT content decreases from 80 through 69 to 50% in the mixture the LC domains in the extrudates occupy a large fraction of the fracture cross-sectional area. This progression of events is shown in the micrographs (from left to right) of Figure 6. However, when the LCP6/4 is the major component in the mixture, the morphology of the extrudate indicates network interpenetration as shown in the micrograph on the extreme right of Figure 6. The features exhibited in the micrograph resemble a series of ridges and crevices. The biphasic character of the extrudate is illustrated by the interpenetration of a smooth surface network with one of a rougher surface by the micrograph.

The influence of the reaction in the melt between PHMT and LCP6/4 upon the morphology of the extrudate is shown in Figure 7. The SEM micrograph of the fracture cross section of the 67PHMT-33LCP6/4 extrudate mixed at 260°C for 200 min (left) is compared to the micrograph of the fracture of the extrudate with the same component content but with 0.6% (weight basis) of DNOP blended for 180 min at 260°C (on the right). Both extrudates have a biphasic morphology. The embedded LC domains have a spherical shape in the extrudate where the reaction was inhibited by the addition of DNOP. In extrudates where a reaction occurs, the morphology of the LC domains is needlelike. The micrograph of the extrudate with 0.6% DNOP mixed at 260°C (Fig. 7 right) resembles that of the extrudate with the same PHMT-LCP6/4

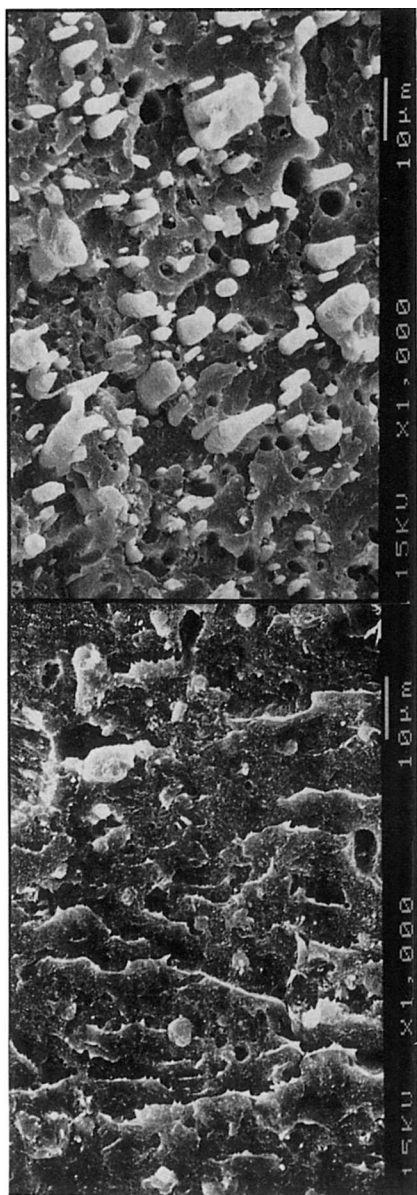
**225****260**

Fig. 5. Micrographs of the fracture cross section of 67PHMT-33LCP6/4 extrudates showing the sensitivity of the morphology to the temperature. The mixtures were reacted at 225 and 260°C.

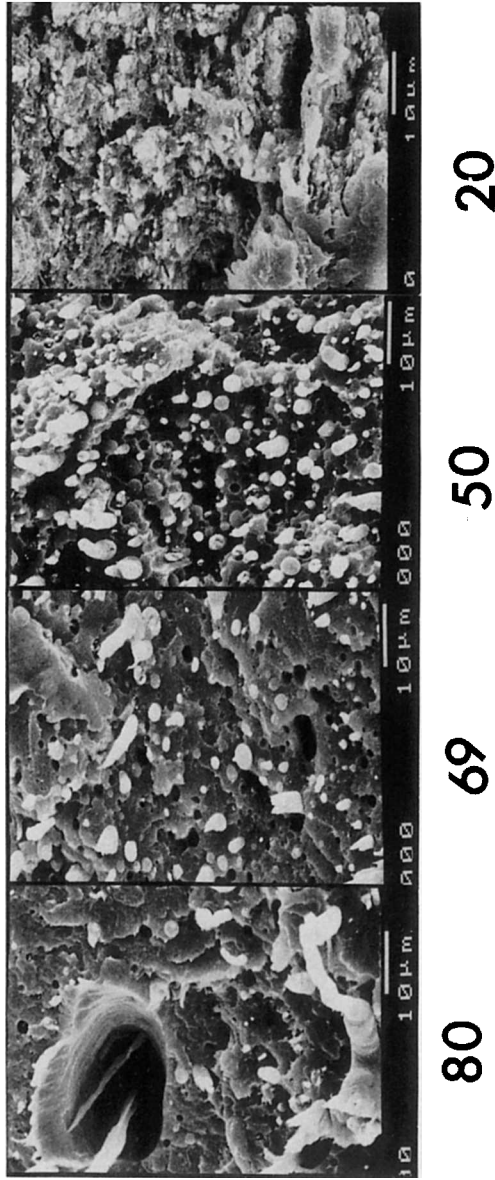
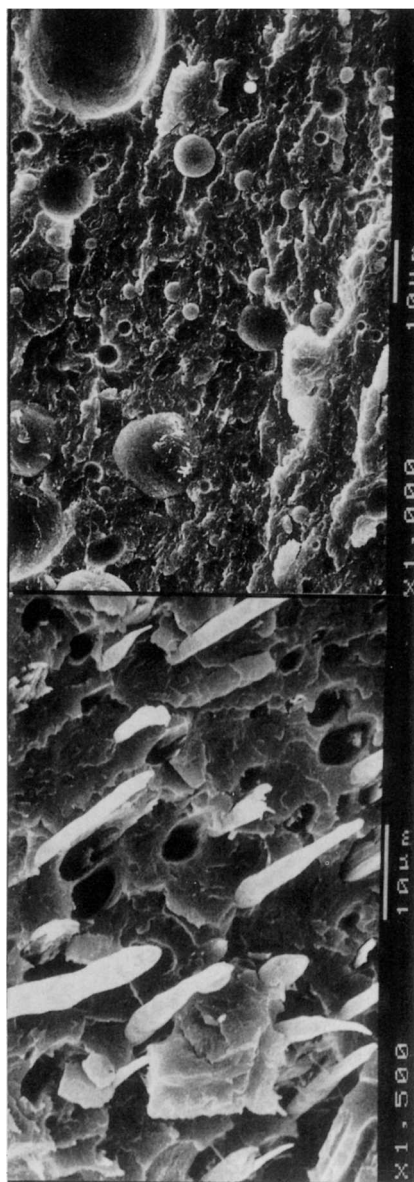


Fig. 6. Micrographs of the fracture cross-section of PHMT-LCP6/4 extrudates mixed at 260°C. The series illustrates the variation of the morphology with mixture concentration. The PHMT content varies from 80% through 67 and 50 to 20% (left to right).



## 67/33 & 0.6% DNOP

Fig. 7. Micrographs of the fracture cross section of extrudates of a 67PHMT-33LCP6/4 mixture reacted for 200 min at 260°C and of a similar mixture with the addition of 0.6% (weight basis) of DNOP. The morphology of the extrudates of the reacted mixture and of the blend when the reaction is inhibited by the addition of DNOP are compared.

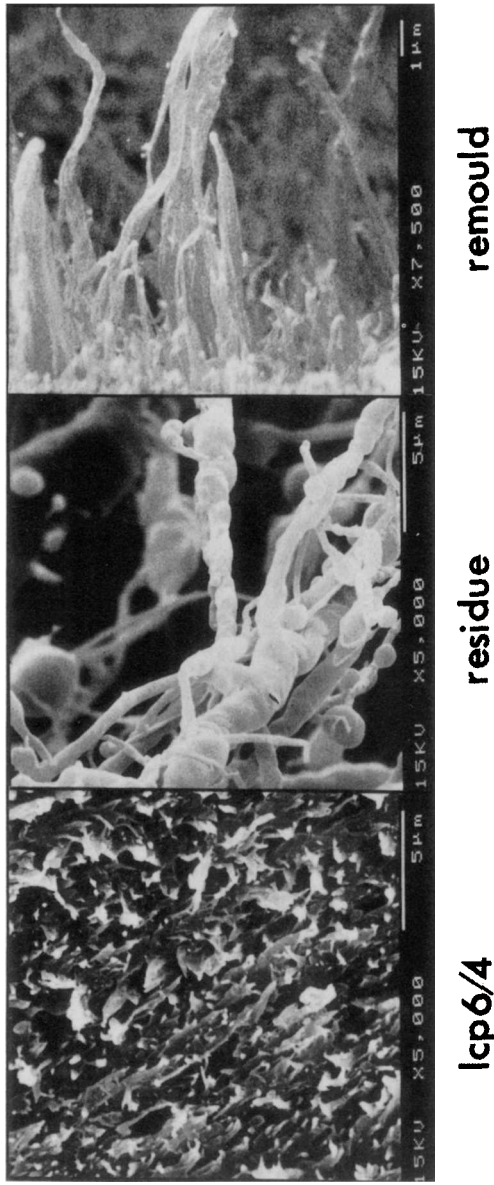


Fig. 8. Micrographs depicting the morphologies of the fracture crosssection of an extrudate of LCP6/4, the residue of a chloroform extracted 33PHMT-67LCP6/4 extrudate reacted for 160 min at 260°C and of a residue remoulded at 260°C and reextruded.



content but was mixed at 225°C (Fig. 5 left). The reaction between PHMT and LCP6/4 is inhibited by a reduction of the reaction temperature or by the addition of DNOP. Regardless of the technique by which the reaction is inhibited, the morphology of the LC domains in the extrudates is spherical, whereas the LC domains in extrudates of reacted mixtures are elongated. A possible explanation for the alteration in the morphology of the embedded LC domains is that the reaction increases the adhesion of the LC domains to the matrix, and that the LC domains are become elongated as the melt flows from the hot molding cavity into the cold tensile bar mold.

The morphological features in the fracture cross sections of a bulk LCP6/4 extrudate, a chloroform extracted residue, and a residue extrudate are compared (left to right) in Figure 8. The chloroform extracted residue fibers (center micrograph) magnified 5000-fold have a nodular appearance. The nodes may be regions where p-OB sequences recombine, or an artifact of the extraction. (The fibrous nature of the residue indicates p-OB sequences of fairly long runs.) Thus the residue was remolded and injected into a mold. The micrograph (Fig. 8, right) of the fibers projecting from the fracture cross section of the residue extrudate (magnified 7500-fold) show that the fibers have a smooth surface. The fibers on the fracture surface of the residue extrudate have a similar appearance to the fibers on a fracture surface of a LCP6/4 extrudate (Fig. 8, left). Thus the nodular appearance (center micrograph) of the chloroform extracted residue apparently is an artifact and does not indicate regions where sequences recombined.

The support of the National Sciences and Engineering Council of Canada is gratefully acknowledged. Sincere thanks to Dr. J. Willis for the scanning electron microscopy work and subsequent analysis and to Ms. D. Thibeault for the NMR spectra.

## References

1. M. Takayanagi, *Polym. J.*, **19**, 21 (1987).
2. G. Kiss, *Polym. Eng. Sci.*, **27**(6), 410 (1987).
3. A. Apicella, P. Iannelli, L. Nicodemo, L. Nicolais, A. Roviello, and A. Sirigu, *Polym. Eng. Sci.*, **26**, 600 (1986).
4. R. A. Weiss, W. Huh, and L. Nicolais, *Polym. Eng. Sci.*, **27**(9), 684 (1987).
5. A. Siegmann, A. Dagan, and S. Kenig, *Polymer*, **26**, 1325 (1985).
6. K. G. Blizard and D. G. Baird, *Polym. Eng. Sci.*, **27**(9), 653 (1987).
7. S. H. Jung and S. C. Kim, *Polym. J.*, **20**(1), 73 (1988).
8. S. K. Sharma, A. Tendolkar, and A. Misra, *Mol. Cryst. Liq. Cryst. Inc. Non. Lin. Opt.*, **157**, 597 (1988).
9. M. Amano and K. Nakagawa, *Polymer*, **28**, 263 (1987).
10. M. Pracella, E. Chiellini, G. Galli, and D. Dainelli, *Mol. Cryst. Liq. Cryst.*, **153**, 525 (1987).
11. M. Kimura and R. Porter, *J. Polym. Sci. Polym. Phys. Ed.*, **22**, 1697 (1984).
12. M. Paci, C. Barone, and P. L. Magagnini, *J. Polym. Sci. Polym. Phys. Ed.*, **25**, 1595 (1987).
13. M. Pracella, D. Dainelli, G. Galli, and E. Chiellini, *Makromol. Chem.*, **187**, 2387 (1986).
14. J. Runt, L. M. Martynowicz-Hans, Du Lei, and M. Mayo, *Am. Chem. Soc. Polym. Prepr.*, **28**(2), 153 (1987).
15. K. Friedrich, M. Hess, and R. Kosfeld, *Makromol. Chem. Macromol. Symp.*, **16**, 251 (1988).
16. S. K. Bhattacharya, A. Tendolkar, and A. Misra, *Mol. Cryst. Liq. Cryst.*, **153**, 501 (1987).
17. E. G. Joseph, G. L. Wilkes, and D. G. Baird, *Am. Chem. Soc. Polym. Prepr.*, **24**(2), 304 (1983).
18. E. G. Joseph, G. L. Wilkes, and D. G. Baird, in *Polymeric Liquid Crystals*, A. Blumstein, Ed., Plenum New York, 1985.

19. T. Kyu and P. Zhuang, *Polym. Commun.*, **29**, 99 (1988).
20. A. Nakai, T. Shiwaku, H. Hasegawa, and T. Hashimoto, *Macromolecules*, **19**, 3008 (1986).
21. G. V. Laivins, *Macromolecules*, **22**, 3974 (1989).
22. A. V. Tobolsky, *Properties and Structure of Polymers*, Wiley, New York, 1960.
23. D. R. Paul, *Adv. Chem. Ser.*, **211**, 3 (1986).
24. J. Devaux, P. Godard, and J. -P. Mercier, *Polym. Eng. Sci.*, **22**(4), 229 (1982).
25. W. J. Jackson Jr. and H. F. Kuhfuss, *J. Polym. Sci. Polym. Chem. Ed.*, **14**, 2043 (1976).
26. H. Muramatsu and W. R. Krigbaum, *J. Polym. Sci. Polym. Phys. Ed.*, **25**, 2303 (1987).
27. W. Meesiri, J. Menczel, U. Gaur, and B. Wunderlich, *J. Polym. Sci. Polym. Phys. Ed.*, **20**, 719 (1982).
28. V. A. Nicely, J. T. Dougherty, and L. W. Renfro, *Macromolecules*, **20**(3), 573 (1987).
29. R. S. Benson and D. N. Lewis, *Polym. Commun.*, **28**, 289 (1987).
30. J. Blackwell, G. Lieser, and G. A. Gutierrez, *Macromolecules*, **16**, 1418 (1983).
31. P. G. Hedmark, J. -F. Jansson, A. Hult, H. Lindberg, and U. W. Gedde, *J. Appl. Polym. Sci.*, **34**, 743 (1987).
32. J. A. Cuculo and G. -Y. Chen, *J. Polym. Sci. Polym. Phys. Ed.*, **26**, 179 (1988).
33. E. G. Joseph, G. L. Wilkes, and D. G. Baird, *Polym. Eng. Sci.*, **25**(7), 377 (1985).
34. M. Aubin and R. E. Prud'homme, *Polym. Sci. Eng.*, **24**(5), 350 (1984).
35. E. Ponnusamy and T. Balakrishnan, *Polym. J.*, **19**(10), 1209 (1987).
36. F. W. Billmeyer Jr., *Textbook of Polymer Science*, 2nd ed., Wiley-Interscience, New York, 1971, 229 pp.
37. F. Pilati, E. Marianucci, and C. Berti, *J. Appl. Polym. Sci.*, **30**, 1267 (1985).
38. H. Watanabe and M. Okada, *Jpn. Kokai*, **72-32**, 295 (1972).
39. J. Devaux, P. Godard, and J. P. Mercier, *J. Polym. Sci. Polym. Phys. Ed.*, **20**, 1875, 1895, 1901 (1982).
40. J. Devaux, P. Godard, J. P. Mercier, R. Touillaux, and J. M. Dereppe, *J. Polym. Sci. Polym. Phys. Ed.*, **20**, 1881 (1982).
41. J. G. Smith, C. J. Kibler, and R. M. Schulken, Jr., U.S. Pat. 3,483,157 (1969).
42. J. P. Mercier, J. Devaux, and P. Godard, Fr. Pat. 2,343,778 (1977).
43. D. Delimoy, C. Bailey, J. Devaux, and R. Legras, *Polym. Eng. Sci.*, **28**(2), 104 (1988).

Received December 19, 1988

Accepted June 21, 1989